Organometallics **2005,** *24,* 1533−1543

Rac/meso Transformations of Disiloxane-bis(1-indenyl)-*ansa*-ferrocenes: An X-ray Crystallographic and NMR Study

Masaaki Amako,[†,‡] Jonathan Schinkel,[†] Michael A. Brook,[*,†] Michael J. McGlinchey,[†,§] and James F. Britten[†]

Department of Chemistry, McMaster University, 1280 Main Street,
W. Hamilton, Ontario, Canada L8S 4M1, and Dow Corning Corporation,
2200 W. Salzburg Road, Midland, Michigan

Received October 20, 2004

Both stereoisomers of disiloxane-bis(1-indenyl)-*ansa*-ferrocene, Fe(η^5-inden-1-yl-SiMe$_2$)$_2$O, **1**, were prepared by the reaction of disiloxane-bis-1,3-inden-1′-yl anion with FeCl$_2$; the diastereomers were separated by column chromatography and recrystallized from *n*-heptane. A single-crystal X-ray diffraction study confirmed that each stereoisomer, *racemic* $\mathbf{1}_r$ and *meso* $\mathbf{1}_m$, involves parallel bis-indenyl coordination to the Fe metal center. These isomers were also characterized by ^{1}H, ^{13}C, and ^{29}Si NMR and IR spectroscopy. Compounds $\mathbf{1}_r$ and $\mathbf{1}_m$ could each be transformed into the other diastereomer: the conversion was retarded by base, but accelerated under weakly acidic conditions. The mechanism of this process, investigated using deuterium labeling experiments, is consistent with a series of successive 1,5-suprafacial, sigmatropic silicon shifts. Compound **1** was also copolymerized with 1,1,3,3,5,5,7,7-octamethylcyclotetrasiloxane (D$_4$) and 1,1,1,3,3,5,5,5-octamethyltrisiloxane (MDM) to produce green organometallic polymers.

Introduction

Over five decades have passed since the discovery of ferrocene.[1] Since that time, related metallocene structures have been extended to multinuclear compounds having Cp ligands, half-sandwich type compounds, bridged Cp ligands generating *ansa*-metallocenes, etc. Particularly relevant to this report are the permethylsilicocene[2] and Fe(η^5-indene)$_2$ derivatives.[3]

Ansa-metallocenes have recently been investigated in two main areas: as olefin polymerization catalysts with the early transition metals at a metal center (Chart 1A),[4−6] and as the basic monomer unit in organometallic polymers prepared by ring-opening polymerization with the late transition metal incorporated as the metal center (Chart 1B).[7,8] In the former case, the metal center is strongly bonded to the Cp ring; in contrast, in the latter case the metal center is relatively weakly coordinated with the carbon rings, so the ligands are very labile. Several groups have described methods that can be used to control metallocene bonding, including the use of a variety of transition metal centers and bridging groups, symmetric stereo properties,[9] chiral substituents on the coordinating rings,[10] and ring strain.[11]

Chart 1. (A) Polymerization of Ferrocenophanes;[11] (B) Metallocene Polymerization Catalysts;[8] (C) Related Metallocene Structures

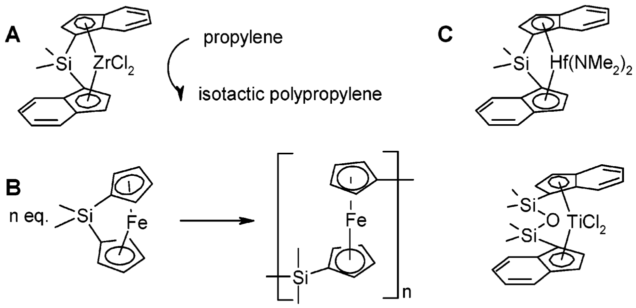

Manners et al. have reported widely on the use of SiR$_2$-bridged [1]-ferrocenophanes as monomers; the resulting polymers, or copolymers, have been targeted to a variety of applications.[11] These workers have also

---

[*] To whom correspondence should be addressed. Fax: +1 905 522 2509. Tel: +1 905 525 9140, ext. 23483. E-mail: mabrook@mcmaster.ca.

[†] McMaster University.

[‡] Dow Corning Corporation.

[§] Current address: Department of Chemistry, University College Dublin, Belfield, Dublin 4, Ireland.

(1) (a) Wilkinson, G.; Rosenblum, M.; Whiting, R. B.; Woodward, R. B. *J. Am. Chem. Soc.* **1952**, *74* 2125. (b) Fisher, E. O.; Pfab, W. *Z. Naturforsch* **1952**, *7B*, 377.

(2) Jutzi, P.; Holtmann, U.; Kanne, D.; Krüger, C.; Blom, R.; Gleiter, R.; Hyla-Kryspin, I. *Chem. Ber.* **1989**, *122*, 1629.

(3) Osiecki, J. H.; Hoffman, C. J. *J. Organomet. Chem.* **1965**, *3*, 107.

(4) For a recent review of the single-site olefin polymerization catalysts, see: (a) Shiono, T.; Nishii, K. *Kobunshi* **2003**, *52*, 908. (b) With stereochemistry: Coates, G. W. *Chem. Rev.* **2000**, *100*, 1223.

(5) For a review of group 4 *ansa*-Cp-amido catalysts for olefin polymerization see: McKnight, A. L.; Waymouth, R. M. *Chem. Rev.* **1998**, *98*, 2587.

(6) Dahlmann, M.; Erker, G.; Nissinen, M.; Fröhlich, R. *J. Am. Chem. Soc.* **1999**, *121*, 2820.

(7) For a general review of organometallic polymers, see: Archer, R. D. *Inorganic and Organometallic Polymer*; Wiley-VCH: New York, 2001.

(8) Mizuta, T.; Onishi, M.; Miyoshi, K. *Organometallics* **2000**, *19*, 5005.

(9) Caporaso, L.; Izzo, L.; Zappile, S.; Oliva, L. *Macromolecules* **2000**, *33*, 7275, and references therein.

(10) Beagley, P.; Davies, P. J.; Blacker, A. J.; White, C. *Organometallics* **2002**, *21*, 5852, and references therein.

(11) For leading reviews, see: (a) Manners, I. *Adv. Organomet. Chem.* **1995**, *37*, 131. (b) Nyuyen, P.; Gòmez-Elipse, P.; Manners, I. *Chem. Rev.* **1999**, *99*, 9, 1515. (c) Hudson, R. D. A. *J. Organomet. Chem.* **2001**, *637−639*, 47.

10.1021/om0491847 CCC: $30.25

reported on disiloxane- and trisiloxane-bridged ferrocenophanes that are significantly less ring strained than the single silicon-containing ferrocenophanes.[12] Pannell et al. have also examined [1]-silaferrocenophanes, their ring-opened polymers,[13] and their applications,[14] explored the nature of ferrocene interactions on diferrocenyl disiloxane complexes,[15] and developed a new ring-opening polymerization of 1-sila-3-metallacyclobutanes.[16] Several other reports of disiloxane-bridged *ansa*-ferrocenes have appeared.[17−19]

Indenyl ligands have also been extensively explored in ferrocenyl-type systems and behave quite differently than the Cp analogues.[20] O'Hare et al. reported the synthesis of ferrocenophanes bearing permethylindenyl groups as the coordination ligands.[21] Jordan et al. have described a variety of *ansa*-metallocene bis(amido) complexes, such as *rac*-(ethylenebis(1-indenyl))Zr(NMe_2)$_2$, *rac*-(Me_2Si(1-indenyl)$_2$)Zr(NMe_2)$_2$, and *rac*/*meso*-(Me_2Si(1-indenyl)$_2$)Hf(NMe_2)$_2$.[22] [*rac*-1,3-Bis(η^5-indenyl)-1,1,3,3-tetramethylsiloxane]dichlorotitanium and -zirconium have also been described, as have bimetallic compounds such as $Fe_2(CO)_2(\mu\text{-}CO)_2(\mu\text{-}\eta^5\text{-inden-1-yl-}SiMe_2)_2O$.[23] However, in all cases, either stereoisomeric mixtures were produced[24] or only one of the isomers was characterized by X-ray crystallography.[21,25]

During the preparation of siloxane-substituted ferrocenophanes, for use as co-monomers, we have been able to isolate both stereoisomers and to demonstrate their interconversion under certain conditions. In this report, we describe both *racemic* and *meso* stereoisomers of nonstrained disiloxane-bis(1-indenyl)-*ansa*-ferrocenes, their transformational behavior, and their copolymerization with oligosiloxanes.

Results and Discussion

Synthesis, Characterization, and General Properties of Disiloxane-bis(1-indenyl)-*ansa*-ferrocenes 1. Disiloxane-bis(1-indenyl)-*ansa*-ferrocenes, **1**, were prepared as shown in Scheme 1 or, alternatively, via treatment of **2** with Na, followed by addition of $FeCl_2$. Both reactions gave almost the same yield (ca. 16%), which was similar to that reported for Fe(η^5-CpSiMe$_2$)$_2$O.[12] Compound **2** was prepared by the treatment of indene with *n*-BuLi, followed by addition of 1,3-dichloro-1,1,3,3-tetramethyldisiloxane.

Scheme 1

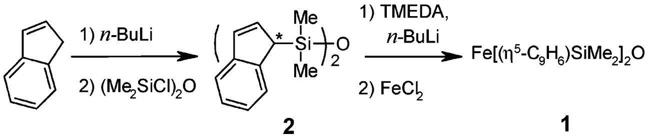

Scheme 2

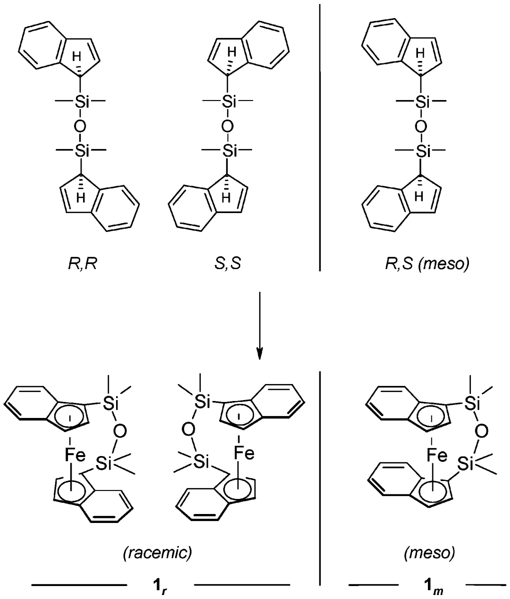

Disiloxane **2** exists as three stereoisomers, as shown in Scheme 2 as a consequence of the stereocenters at the 1-position on each indenyl ring, as indicated in Scheme 1. The diastereomers of **2** could not be separated by column chromatography, but crude **1** was obtained as a black-green solid that was shown by ^{1}H NMR spectroscopy (vide infra) to be a 70:30 mixture of *racemic* and *meso* isomers. Each *ansa*-ferrocene diastereomer, $\mathbf{1}_r$ and $\mathbf{1}_m$, was successfully isolated by column chromatography on alumina; subsequent recrystallization from *n*-heptane allowed unequivocal characterization by single-crystal X-ray diffraction and multinuclear magnetic resonance techniques. Compounds $\mathbf{1}_r$ and $\mathbf{1}_m$ readily dissolved in most aromatic and aliphatic hydrocarbon organic solvents and yielded dark blue and dark green solutions, respectively.

Compounds $\mathbf{1}_r$ and $\mathbf{1}_m$ were characterized initially by NMR (see Table 1 and Supporting Information). The protons on the five-membered ring of $\mathbf{1}_r$ (the major isomer) resonate at higher field (lower frequency) relative to their $\mathbf{1}_m$ counterparts, presumably because of the shielding effect of the six-membered ring of the other indenyl ligand. The ^{1}H NMR assignments of the 2- and

---

(12) Angelakos, C.; Zamble, D. B.; Foucher, D. A.; Lough, A. J.; Manners, I. *Inorg. Chem.* **1994**, *33*, 1709.

(13) (a) Pannell, K. H.; Dementiev, V. V.; Li, H.; Cervantes-Lee, F.; Nguyen, M. T.; Diaz, A. F. *Organometallics* **1994**, *13*, 3644. (b) Papkov, V. S.; Gerasimov, M. V.; Dubovik, I. I.; Sharma, S.; Dementiev, V. V.; Pannell, K. H. *Macromolecules* **2000**, *33*, 7107. (c) Nyugen, M. T.; Diaz, A. F.; Dementiev, V. V.; Pannell, K. H. *Chem. Mater.* **1993**, *5*, 1389.

(14) (a) Espada, L.; Pannell, K. H.; Papkov, V.; Leites, L.; Bukalov, S.; Suzdalev, I.; Tanaka, M.; Hayashi, T. *Organometallics* **2002**, *21*, 3758. (b) Espada, L. I.; Shadaram, M.; Robillard, J.; Pannell. K. H. *J. Inorg. Organomet. Polym.* **2000**, *10*, 169.

(15) Cervantes-Lee, F.; Sharma, H. K.; Pannell, K. H.; Derecskei-Kovacs, A.; Marynick, D. S. *Organometallics* **1998**, *17*, 3701.

(16) Sharma, H. K.; Cervantes-Lee, F.; Pannell, K. H. *J. Am. Chem. Soc.* **2004**, *126*, 1326.

(17) Kumada, M.; Kondo, T.; Mimura, K.; Yamamoto, K.; Ishikawa, M. *J. Organomet. Chem.* **1972**, *43*, 307.

(18) Schaaf, R. L.; Kan, P. T.; Lenk, C. T. *J. Org. Chem.* **1961**, *26*, 1790.

(19) Hartinger, C.; Brehmer, T. H.; Giester, G.; Galanski, M.; Nazarov, A. A.; Luther, S. M.; Keppler, B. K. *Inorg. Chim. Acta* **2002**, *328*, 237.

(20) Zhang, Z.; Sanchez, R.; Pannell, K. H. *Organometallics* **1996**, *14*, 2605−2608.

(21) Alías, F. M.; Barlow, S.; Tudor, J. S.; O'Hare, D.; Perry, R. T.; Nelson, J. M.; Manners, I. *J. Organomet. Chem.* **1997**, *528*, 47.

(22) (a) Christopher, J. N.; Jordan, R. F.; Peterson, J. L.; Young, V. G. *Organometallics* **1997**, *16*, 3044. (b) Diamond, G. M.; Jordan, R. F.; Peterson, J. L. *J. Am. Chem. Soc.* **1996**, *118*, 8024. (c) Christopher, J. N.; Diamond, G. M.; Jordan, R. F.; Peterson, J. L. *Organometallics* **1996**, *15*, 4038. (d) Diamond, G. M.; Jordan, R. F.; Peterson, J. L. *Organometallics* **1996**, *15*, 4030. (e) Diamond, G. M.; Jordan, R. F.; Peterson, J. L. *Organometallics* **1996**, *15*, 4045. (f) Diamond, G. M.; Rodewald, S.; Jordan, R. F. *Organometallics* **1995**, *14*, 5.

(23) Wang, B. Q.; Xu, S. S.; Zhou, X. Z. *Polyhedron* **1997**, *16*, 2737.

(24) Song, W.; Shackett, K.; Chien, J. C. W.; Rausch, M. D. *J. Organomet. Chem.* **1995**, *501*, 375.

(25) Naderer, H.; Siebel, E.; Fischer, R. D. *J. Organomet. Chem.* **1996**, *518*, 181.

Table 1. Selected NMR Data for $\mathbf{1}_r$ and $\mathbf{1}_m$

	$\mathbf{1}_r$		$\mathbf{1}_m$	
^{1}H NMR in	toluene-d_8	CD_2Cl_2	toluene-d_8	CD_2Cl_2
SiMe	0.50,0.58	0.47,0.57	0.41,0.52	0.42, 0.50
H(2)	2.68	2.67	3.99	4.22
H(3)	4.42	4.51	4.80	5.11
H(6),	7.64	7.65	6.50	6.50
H(9)	7.69	7.79	6.70	6.59
H(7), H(8)	6.87	7.01	6.73	6.72
^{13}C NMR in	CD_2Cl_2		CD_2Cl_2	
SiMe	0.7, 1.4		0.8, 1.4	
C(1)	64.6		63.0	
C(2)	81.1		75.7	
C(3)	67.8		64.7	
C(4), C(5)	87.4, 90.4		90.6, 92.1	
C(6)	131.2		126.4	
C(7), C(8)	124.2, 124.6		122.3, 122.6	
C(9)	130.0		125.3	
^{29}Si NMR in	$CDCl_3$	CD_2Cl_2	$CDCl_3$	CD_2Cl_2
	1.32	−0.16	1.60	0.16

Chart 2. ^{1}H NOE and ^{1}H−^{29}Si HMBC Interactions Observed in $\mathbf{1}_r$ and $\mathbf{1}_m$

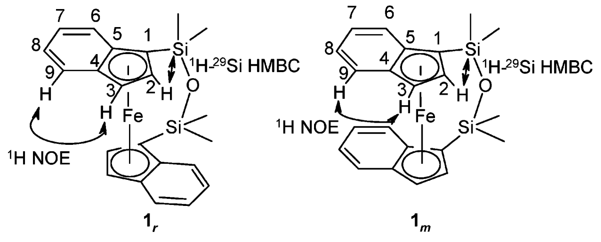

3-positions of the indenyl ring were elucidated on the basis of ^{1}H NOE and ^{1}H−^{29}Si HMBC experiments (Chart 2). Thus, the strong correlation between the peaks at δ 4.51 (H-3) and 7.79 (H-9) in $\mathbf{1}_r$ reveals the locations of these protons in the five- and six-membered rings. Likewise, one can assign the resonances at δ 5.11 (H-3) and 6.59 (H-9) in $\mathbf{1}_m$. Moreover, in the ^{1}H−^{29}Si HMBC spectra, a three-bond correlation connects the δ 2.67 (H-2) peak of $\mathbf{1}_r$ with the ^{29}Si signal at δ −0.16; the corresponding ^{1}H and ^{29}Si values for $\mathbf{1}_m$ are δ 4.22 and 0.16, respectively. ^{13}C NMR spectra were assigned by ^{1}H−^{13}C gradient HSQC and ^{1}H−^{13}C HMBC spectra (in CD_2Cl_2). The IR spectrum of $\mathbf{1}_r$ exhibits a strong Si−O stretching vibration at 1016 cm^{-1}, while in $\mathbf{1}_m$ two signals (at 1022 and 1006 cm^{-1}) were found. Overall, these spectroscopic features are consistent with the assignments of the products as $\mathbf{1}_r$, which possesses a C_2 axis, and $\mathbf{1}_m$, in which the iron and oxygen atoms lie on a molecular mirror plane.

Table 2. Selected Bond Lengths (Å) and Angles (deg) for $\mathbf{1}_r$ and $\mathbf{1}_m$

	$\mathbf{1}_r$	$\mathbf{1}_m$
Fe(1)−C(1)	2.057(5)	2.049(5)
Fe(1)−C(2)	2.035(5)	2.037(5)
Fe(1)−C(3)	2.045(5)	2.045(5)
Fe(1)−C(4)	2.094(5)	2.096(4)
Fe(1)−C(5)	2.088(5)	2.090(4)
Fe(1)−C(10)	2.059(5)	2.069(4)
Fe(1)−C(11)	2.035(5)	2.044(5)
Fe(1)−C(12)	2.056(5)	2.050(5)
Fe(1)−C(13)	2.095(5)	2.110(5)
Fe(1)−C(14)	2.081(5)	2.078(5)
Si(1)−O(1)	1.626(4)	1.643(3)
Si(2)−O(1)	1.640(4)	1.637(4)
Si(1)−C(1)	1.850(5)	1.874(5)
Si(2)−C(10)	1.848(6)	1.862(5)
C(1)−C(2)	1.427(7)	1.439(7)
C(1)−C(5)	1.464(7)	1.445(7)
C(2)−C(3)	1.412(7)	1.414(7)
C(3)−C(4)	1.440(7)	1.428(7)
C(4)−C(5)	1.449(7)	1.461(7)
C(4)−C(9)	1.437(7)	1.426(7)
C(5)−C(6)	1.433(7)	1.415(7)
C(6)−C(7)	1.345(7)	1.376(7)
C(7)−C(8)	1.417(8)	1.425(8)
C(8)−C(9)	1.351(7)	1.348(8)
C(10)−C(11)	1.425(7)	1.439(7)
C(10)−C(14)	1.458(7)	1.454(7)
C(11)−C(12)	1.409(7)	1.411(7)
C(12)−C(13)	1.443(7)	1.425(7)
C(13)−C(14)	1.441(7)	1.446(7)
C(13)−C(18)	1.431(7)	1.430(7)
C(14)−C(15)	1.438(7)	1.429(7)
C(15)−C(16)	1.346(7)	1.371(7)
C(16)−C(17)	1.415(7)	1.419(8)
C(17)−C(18)	1.336(7)	1.347(8)
C(1)−Si(1)−O(1)	111.2(2)	108.9(2)
C(19)−Si(1)−O(1)	108.5(3)	108.5(3)
C(20)−Si(1)−O(1)	106.7(3)	105.9(2)
C(1)−Si(1)−C(19)	109.6(3)	112.2(3)
C(1)−Si(1)−C(20)	111.3(3)	109.3(3)
C(19)−Si(1)−C(20)	109.5(3)	111.9(3)
C(10)−Si(2)−O(1)	109.5(2)	110.6(2)
C(21)−Si(2)−O(1)	106.8(2)	106.7(3)
C(22)−Si(2)−O(1)	109.2(2)	109.2(3)
C(10)−Si(2)−C(21)	109.6(3)	108.5(3)
C(10)−Si(2)−C(22)	109.7(3)	112.5(3)
C(21)−Si(1)−C(22)	112.1(3)	109.2(4)
Si(1)−O(1)−Si(2)	140.7(2)	139.1(2)

The structures were secured unequivocally by X-ray crystallography. A black single crystal of $\mathbf{1}_r$, isolated from n-heptane, was mounted on the top of a glass fiber over a plate cooled to dry ice temperature: analogously, a dark red single crystal of $\mathbf{1}_m$ was isolated from n-heptane. The molecular structures are shown in Figure 1, and bond lengths and angles may be found in Table 2. With compound $\mathbf{1}_m$, two independent molecules

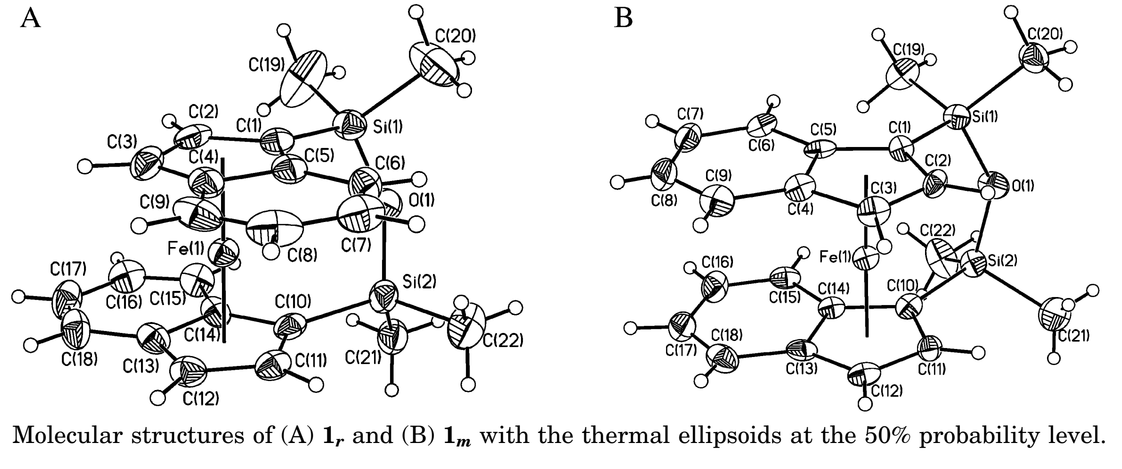

Figure 1. Molecular structures of (A) $\mathbf{1}_r$ and (B) $\mathbf{1}_m$ with the thermal ellipsoids at the 50% probability level.

Table 3. Crystallographic Data for 1_r and 1_m

	1_r (CDCC 252723)[41]	1_m (CDCC 252722)[41]
chemical formula	$C_{22}H_{24}Fe_1O_1Si_2$	
fw	416.44	
solvent	*n*-heptane	*n*-heptane
cryst color, habit	black needle	dark red plate
cryst syst	orthorhombic	triclinic
space group	*Pbca*	$P\bar{1}$
a (Å)	14.165(7)	11.417(3)
b (Å)	16.231(9)	16.838(4)
c (Å)	17.570(10)	10.436(3)
α (deg)	90	88.025(3)
β (deg)	90	89.479(3)
γ (deg)	90	86.487(5)
volume (Å^3)	4040(4)	2001.2(9)
D(calcd) (g cm^{-3})	1.369	1.382
λ (Å)	0.71073	0.71073
radiation	Mo Kα	Mo Kα
monochromator	graphite	graphite
temperature (K)	173(2)	173(2)
Z	8	4
cryst size (cm^3)	0.22 × 0.07 × 0.02	0.60 × 0.30 × 0.08
abs coeff (μ) (mm^{-1})	0.873	0.882
min./max. transmn	0.654	.734
absorption correction	Multiscan, SADABS	
diffractometer	Bruker P4, Smart1K CCD, rotating anode	
diffraction geometry	Φ and ω scans	
2θ max (deg)	45.0	50.7
hkl range	±15, ±17, ±18	±13, ±20, ±12
no. reflns collected	22 670	15 386
no. indep reflns	2637	7298
R(int)	0.1583	0.0585
R1 ($I > 2\sigma(I)$)	0.0554	0.0567
wR2 ($I > 2\sigma(I)$)	0.0845	0.1230
R1 (all data)	0.1116	0.1105
wR2 (all data)	0.0987	0.1441

having only minor geometric differences were found in the crystal with the centrosymmetric space group $P\bar{1}$ (only one is shown). Compound $\mathbf{1}_r$, by contrast, crystallizes in space group *Pbca* and contains eight molecules—four pairs of (*R*,*R*) and (*S*,*S*) enantiomers—in the unit cell and is thus racemic (Table 3).

The indenyl carbon atoms in each stereoisomer of $\mathbf{1}_r$ and $\mathbf{1}_m$ showed a mean deviation of less than 0.02 Å for both compounds; that is, the indenyl ligands are virtually planar. The tilt angles between the two indenyl ligands coordinated to the iron of $\mathbf{1}_r$ and $\mathbf{1}_m$ were 2.1(1)° and 2.8(2)°, respectively. The almost perfectly parallel arrangement of the pairs of indenyl ligands in both compounds is also reflected in the angle between the centroids of the two five-membered indenyl rings through the iron metal center, which was 179° for both compounds.

Previous reports of structurally related compounds include *racemic* $O(SiMe_2\text{-}\eta^5\text{-1-indenyl})_2ZrCl_2$[25] and *racemic* $SiMe_2(\eta^5\text{-1-permethylindenyl})_2Fe$,[21] in which the angles between the two indenyl planes were 52° and 13°, respectively; the angles through the metal were 131° and 171°, respectively. The angles in the zirconium complex reflect the pseudo-tetrahedral coordination at the metal center. Analogous Cp-substituted compounds exhibited values for Cp−M−Cp of 130.9° ($O(SiMe_2\text{-}\eta^5\text{-}Cp)_2ZrCl_2$)[26] and 130.8° ($O(SiMe_2\text{-}\eta^5\text{-}Cp)_2TiCl_2$).[27]

The remaining structural features in $\mathbf{1}_r$ and $\mathbf{1}_m$ are consistent with those in related compounds. The average

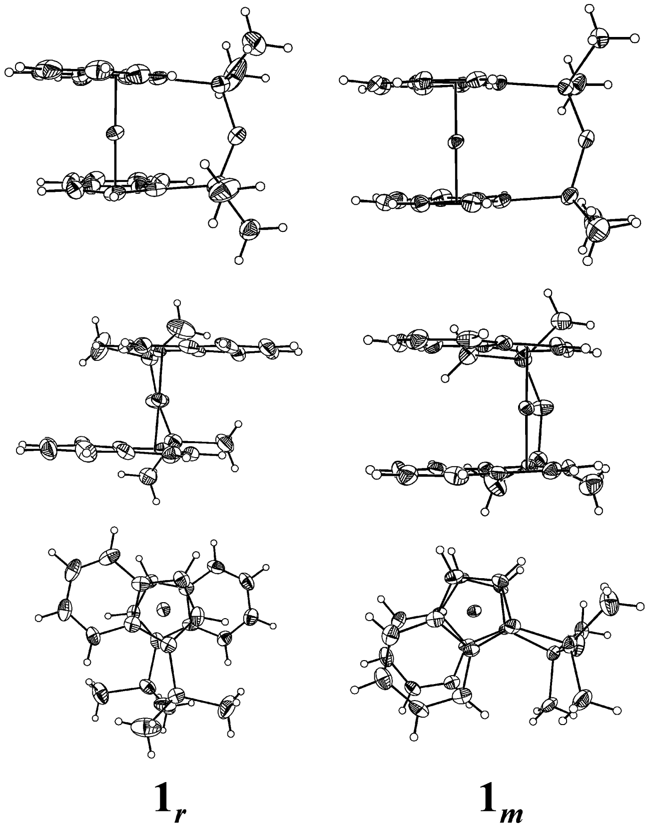

Figure 2. Alternative views of $\mathbf{1}_r$ (left) and $\mathbf{1}_m$ (right), with the thermal ellipsoids at the 50% probability level.

Si−*ipso* C distances of $\mathbf{1}_r$ and $\mathbf{1}_m$ were 1.849 and 1.871 Å, respectively, similar to those in $Cl_2Zr(\eta^5\text{-inden-1-yl-}SiMe_2)_2O$, 1.871 Å,[25] and $Fe(\eta^5\text{-}Cp_2)SiMe_2$, 1.858 Å,[28] but shorter than in $Fe(\eta^5\text{-}C_9Me_6)_2SiMe_2$, 1.904 Å.[21] In addition, all angles and bond lengths around each Si and O atom were within normal ranges and comparable those reported in $O(SiMe_2\text{-}\eta^5\text{-}Cp)_2Fe$ (Table 2).[12]

Interconversion of $\mathbf{1}_r$ and $\mathbf{1}_m$. While the observation of late transition metal *rac*-indenyl metallocenes is quite general, the ability to characterize both *rac*- and *meso*-isomers by X-ray crystallography, as depicted in Figure 2, is rare. This provides an opportunity to examine structural interchange between the isomers. Although $\mathbf{1}_r$ and $\mathbf{1}_m$ were stable as crystalline solids under an inert atmosphere at ambient temperature for at least six months, each one is slowly transformed to the other isomer at 110 °C in toluene-d_8. When crystals of $\mathbf{1}_r$ and $\mathbf{1}_m$ were each separately dissolved in toluene-d_8 in a flame-sealed tube, the ^1H NMR spectrum of each compound, $\mathbf{1}_r$ and $\mathbf{1}_m$, was monitored over an 18 day period, as shown in Figure 3A/B. The small peaks labeled $\mathbf{1}_X$ indicate the formation of a new, likely isomeric, compound that could not be isolated, but which was tentatively assigned as $Fe[(\eta^5\text{-inden-2-yl})SiMe_2]_2O$ (see Figure 4C) based on its ^1H NMR (δ 0.04 (s, 6H), 0.36 (s, 6H), 3.40 (br s, 2H), 3.42 (br s, 2H) 7.12 (m, 2H), 7.16 (m, 2H), 7.40 (d, *J* = 7.1 Hz, 2H), 7.48 (d, *J* = 7.0 Hz, 2H)) and $^1H-^1H$ COSY spectra (each combination of δ 7.12 and 7.48, δ 7.16 and 7.40 had strong correlations, but δ 3.40 and 3.42 did not have any strong

---

(26) Ciruelos, S.; Cuenca, T.; Gómez-Sal, P.; Manzanero, A.; Royo, P. *Organometallics* **1995**, *14*, 177.

(27) Curtis, M. D.; D'Errico, J. J.; Duffy, D. N.; Epstein, P. S.; Bell, L. G. *Organometallics* **1983**, *2*, 1808.

(28) Finckh, W.; Tang, B.-Z.; Foucher, D. A.; Zamble, D. B.; Ziembinski, R.; Lough, A. J.; Manners, I. *Organometallics* **1993**, *12*, 823−829.

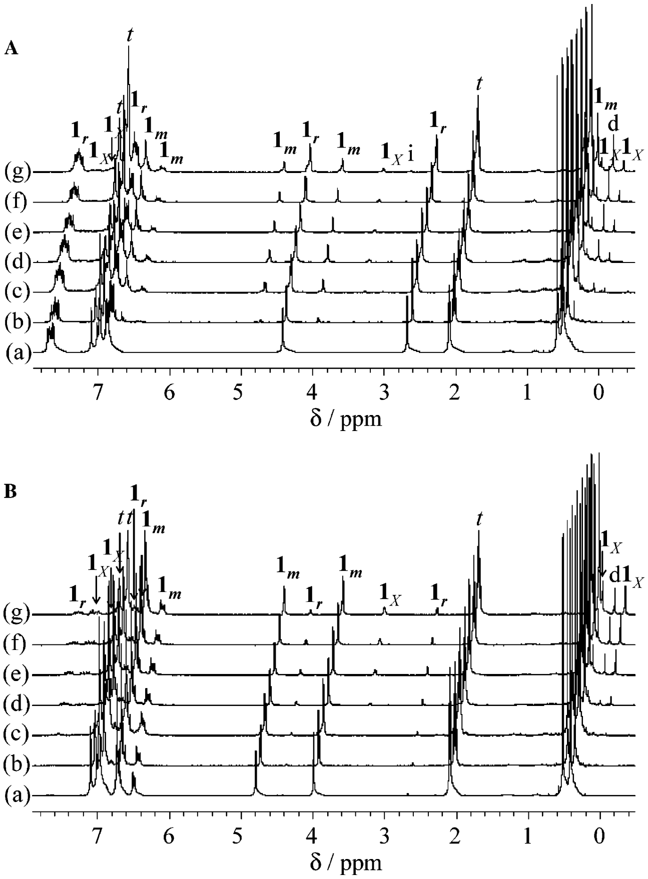

Figure 3. ^{1}H NMR spectra recorded at room temperature of $\mathbf{1}_r$ (A) and $\mathbf{1}_m$ (B) over time at 110 °C in toluene-d_8 (t: toluene, d: hexamethylcyclotrisiloxane): (a) initial, (b) 10 h, (c) 2 days, (d) 4 days, (e) 8 days, (f) 13 days, (g) 18 days.

correlations with other signals). These data are consistent with a molecule of C_2 symmetry, analogous to the bird's eye view of $\mathbf{1}_r$ shown as the lowest structure in Figure 2, except that the benzo moieties are each attached to their neighboring five-membered ring across the C3−C4 positions rather that at the C2−C3 linkage. Such a view clearly illustrates the diastereotopic nature of the trimethylsilyl groups and of the protons in the five- and six-membered rings, which each occurs in pairs.[29]

The ^{29}Si NMR spectra from ^{1}H−^{29}Si HMBC spectra showed a signal at δ −0.8 from the correlation of Si*Me* groups, consistent with silicon being located in close proximity to iron. Over the course of these experiments, trace amounts of two other compounds gradually appeared in Figure 3A/B: the minuscule signal labeled 'i' can be attributed to indene,[30] while the peak 'd' is probably cyclo-1,1,3,3,5,5-hexamethyltrisiloxane (D_3), based on the absence of correlations with any other signal from gradient ^{1}H−^{1}H COSY spectra and its distinctive signal at δ −8.8 ppm in ^{29}Si NMR (from ^{1}H−^{29}Si HMBC spectrum).[31] These features, excluding indene and D_3, were converted into Figure 4, which shows the extent of isomerization as a function of molar concentration/time.

Even in the absence of catalysts, slow interconversion of $\mathbf{1}_r$ to $\mathbf{1}_m$ and from $\mathbf{1}_m$ to $\mathbf{1}_r$ was observed. However, because of the difficulty in obtaining significant amounts of the minor product $\mathbf{1}_m$ in pure form, the investigation of the transformational behavior was mostly performed with $\mathbf{1}_r$. To gain information about the mechanism of the reaction, the effects of a range of solvents and reagents on the rate and extent of interconversion were examined.

As shown in Figure 5, the interconversion of $\mathbf{1}_r \rightarrow \mathbf{1}_m$ was accelerated when THF, which can function as a weakly coordinating ligand, was used as the cosolvent. However, even after 500 h, it is evident that a 1:1 ratio of $\mathbf{1}_r$:$\mathbf{1}_m$ had not been reached.

The effects of acids and bases were also investigated. The exchange between $\mathbf{1}_r$ and $\mathbf{1}_m$ occurred more slowly in the presence of a base, NEt_3 (Figure 6A). In contrast, when $CHCl_3$ was added to $\mathbf{1}_r$, the rate of the exchange reaction to produce $\mathbf{1}_m$ increased, with concomitant formation of $\mathbf{1}_\mathbf{X}$ (Figure 6B). To examine the possible involvement of radicals in this process, the radical trap 2,6-di-*tert*-butyl-4-methylphenol (butylated hydroxytoluene, BHT) was used, but this also led to rearrangement (vide infra). Suspecting that the reaction in $CHCl_3$ might be a consequence of the presence of traces of strong acid, HCl, in the $CHCl_3$, further experiments with weaker acids were undertaken.

Compound $\mathbf{1}_r$ decomposed on contact with acetic acid to generate a precipitate. However, the very weak acids 2,4,6-trimethylphenol and 2,6-di-*tert*-butyl-4-methylphenol (BHT) could be used to catalyze the interconversion. Use of 2,4,6-trimethylphenol led to a significant amount of decomposition, including formation of $\mathbf{1}_X$ and indene, after 200 h. In contrast, BHT accelerated the transformation and led to a final 50:50 product mix of $\mathbf{1}_r$:$\mathbf{1}_m$ (Figure 7); moreover, the rate at which the equilibrium distribution was reached was proportional to the concentration of BHT.

Since the interconversion was acid-catalyzed and base-retarded, we attempted to follow the proton transfer on the NMR time scale using ^{1}H−^{1}H EXSY.[32] Unfortunately, no correlation was observed after several attempts utilizing different mixing times (0.5, 1, 2, 5 s). Therefore, labeling experiments were performed using deuterated-BHT prepared by the reaction of BHT with MeOD to give 88% *d*-BHT (% *d* was calculated from residual H in the ^{1}H NMR). During the transformation with $\mathbf{1}_m$ and *d*-BHT, the deuterium content decreased with time.[33]

Compounds $\mathbf{1}_r$ and $\mathbf{1}_m$, respectively, were allowed to react with *d*-BHT in toluene-d_8 for one month, after which time the solvent was removed and exchanged for freshly distilled toluene for ^{2}H NMR. We were unable to obtain any clear information with $\mathbf{1}_r$ as starting material, but a signal at 4.4 ppm was observed when

---

[29] Although this molecule could, in principle, adopt a time-averaged C_{2v} structure, the room-temperature spectrum suggests that interconversion of the enantiomers of $\mathbf{1}_X$ is slow on the NMR time scale. Indeed, since peak coalescences have not occurred at 300 K, the Gutowsky−Holm approximation yields a barrier of at least 16 kcal mol^{-1}.

[30] ^{1}H NMR spectra (300 MHz, toluene-d_8) of indene: δ 3.03(m, 2H), 6.24 (dt, J = 5.3, 2.0 Hz, 1H), 6.70 (dtd, J = 5.3, 2.0, 0.7 Hz, 1H), 7.10 (m, 1H), 7.16 (m, 1H), 7.24 (m, 1H), 7.27 (m, 1H).

[31] Even if these experiments were operated using anhydrous toluene-d_8 distilled over Na, a trace amount of water could have been present from the sample preparations. After a couple of months, a small amount of ochre-colored solid was found in the bottom of the sample tubes.

[32] Stradiotto, M.; Hughes, D. W.; Bain, A. D.; Brook, M. A.; McGlinchey, M. J. *Organometallics* **1997**, *16*, 5563.

[33] See Figure 3S in the Supporting Information.

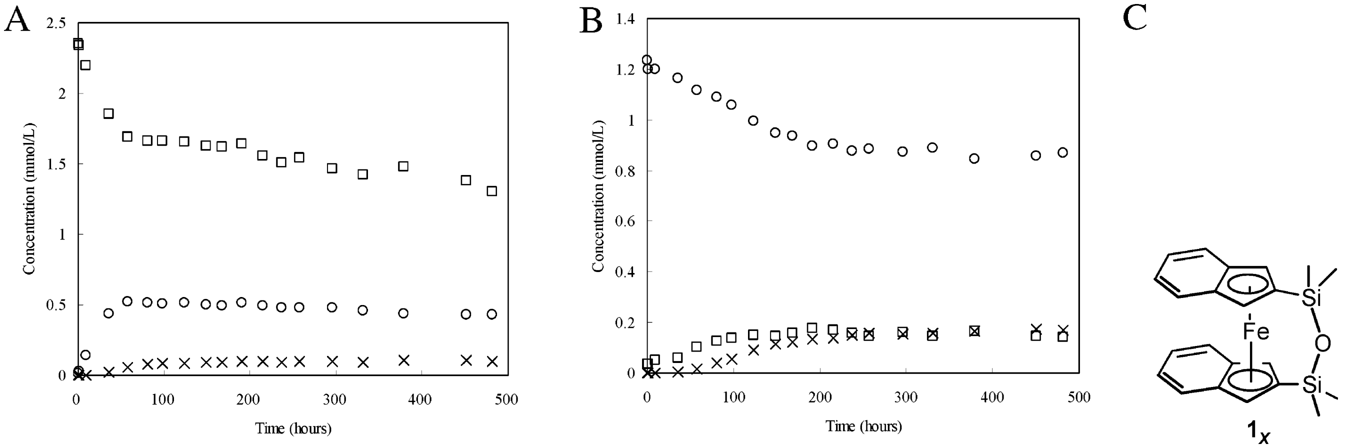

Figure 4. (A) Transformation reaction from $\mathbf{1}_r$ (□: $\mathbf{1}_r$, ○: $\mathbf{1}_m$, ×: $\mathbf{1}_X$). (B) Transformation reaction from $\mathbf{1}_m$. (C) Proposed structure of $\mathbf{1}_X$.

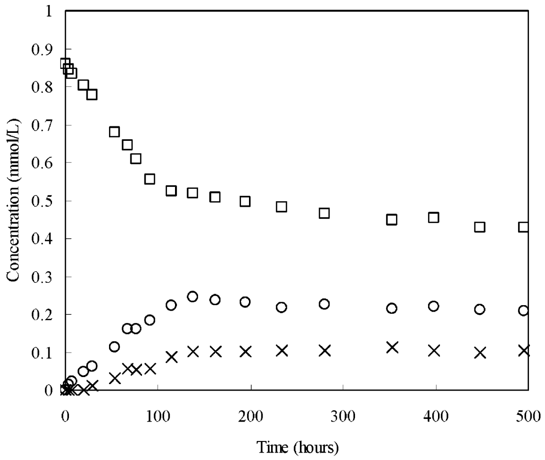

Figure 5. Transformation reaction from $\mathbf{1}_r$ with 2.7 equiv of THF (□: $\mathbf{1}_r$, ○: $\mathbf{1}_m$, ×: $\mathbf{1}_X$).

starting from $\mathbf{1}_m$ (Figure 8). These data suggest that ^{2}H can be introduced at the indenyl 3-position, but not at the 2-position.

Several processes are taking place under the reaction conditions: interconversion of $\mathbf{1}_m$ and $\mathbf{1}_r$ (major), conversion of $\mathbf{1}_m/\mathbf{1}_r$ into $\mathbf{1}_X$ (minor), and protiodesilylation leading to the formation of indene (minor): all three processes are acid-catalyzed. An analysis of all the processes described above demonstrates that in the latter reaction $\mathbf{1}_X$ is preferentially derived from $\mathbf{1}_m$. This is most clear from the reaction with $CHCl_3$ (Figure 6B), where $\mathbf{1}_m$ is first formed from $\mathbf{1}_r$ and then converted to $\mathbf{1}_X$. There is no indication of the presence of $\mathbf{1}_X$ in reactions catalyzed by base, whereas it is formed in higher yield in acid-catalyzed reactions.

Two mechanisms for the $\mathbf{1}_m/\mathbf{1}_r$ interconversion reaction immediately present themselves: metal migration onto the opposite face of the indenyl ligand,[34] and ring slippage of the metal to the aromatic ring, accompanied by sigmatropic rearrangement of the silyl group. The latter is consistent with the outcomes of the processes described above.

Silylated indenes undergo facile sigmatropic rearrangements at elevated temperatures.[35] These rearrangements are generally understood to arise from *suprafacial* 1,5- rather than *antarafacial* 1,3-migrations, which are geometrically much more difficult to achieve. Two sequential 1,5-silyl sigmatropic shifts, via **4**, invert the chirality at one indenyl center, resulting in the interconversion of $\mathbf{1}_m$ and $\mathbf{1}_r$.[36] The barrier to these sigmatropic rearrangements is much lower than that for H migration[35,37] or of transition metals. However, to permit the sigmatropic reaction to occur on the *ansa*-silylferrocene, protonation on the five-membered ring of the indene must be accompanied by a haptotropic shift of the iron from the five- to the six-membered ring, a well-established phenomenon.[38] Metal slippage for late transition metal indenyl complexes from η^5, to η^3, to η^1, depending on electron density on the metal centers, is well precedented.[39] The protonation process will clearly be assisted by the presence of acids and is supported by the reaction with the deuterium-labeled BHT. The acids cannot be too strong, or efficient conversion to $\mathbf{1}_X$ and protiodesilylation to indene occurs.

We thus rationalize the interconversion reaction by the sequence $\mathbf{1}_r \rightarrow \mathbf{3} \rightarrow \mathbf{4} \rightarrow \mathbf{5} \rightarrow \mathbf{1}_m$ (Scheme 3). Protonation and haptotropic shift of Fe is followed by sequential 1,5-sigmatropic shifts and finally deprotonation and metal migration back to the five-membered ring. One can envisage a side process draining the interconversion, forming $\mathbf{1}_X$ from one of the protonated

---

[34] (a) Cotton, F. A. *Acc. Chem. Res.* **1968**, *1*, 257. (b) Cotton, F. A. In *Dynamic Nuclear Magnetic Resonance Spectroscopy*; Jackman, L. M., Cotton, F. A., Eds.; Academic: New York, 1975; Chapter 10, pp 378−398. (c) Mann, B. E. In *Comprehensive Organometallic Chemistry*; Wilkinson, G., Stone, F. G. A., Abel, E. W. Eds.; Pergamon: Oxford, 1982; Chapter 20, pp 89−125.

[35] (a) Grimmond, B. J.; Corey, J. Y. *Organometallics* **1999**, *18*, 4646. (b) Rigby, S. S.; Girard, J.; Bain, A. D.; McGlinchey, M. J. *Organometallics* **1995**, *14*, 3798. (c) Rigby, S. S.; Gupta, H. K.; Werstiuk, N. H.; Bain, A. D.; McGlinchey, M. J. *Polyhedron* **1995**, *14*, 2787. (d) Larrabee, R. B.; Dowden, B. F. *Tetrahedron Lett.* **1970**, 915. (e) Davison, A.; Rakita, P. E. *J. Organomet. Chem.* **1970**, *23*, 407. (f) Davison, A.; Rakita, P. E. *Inorg. Chem.* **1969**, *5*, 1164. (g) Ashe, A. J., III. *Tetrahedron Lett.* **1970**, 2105. (h) Sergeyev, N. M.; Grishin, Yu. K.; Lulikov, Yu N.; Ustynyuk, Yu A. *J. Organomet. Chem.* **1972**, *38*, C1. (i) Lulikov, Yu. N.; Sergeyev, N. M.; Ustynyuk, Yu. A. *J. Organomet. Chem.* **1974**, *65*, 303. (j) McMaster, A. D.; Stobart, S. R. *J. Am. Chem. Soc.* **1982**, *104*, 2109. (k) McMaster, A. D.; Stobart, S. R. *J. Chem. Soc., Dalton Trans.* **1982**, 2275.

[36] Stradiotto, M.; Brook, M. A.; McGlinchey, M. J. *J. Chem. Soc., Perkin Trans. 2* **2000**, 611.

[37] Spangler, C. W. *Chem. Rev.* **1976**, *76*, 187.

[38] Treichel, P. M.; Johnson, J. W. *J. Organomet. Chem.* **1975**, *88*, 207.

[39] (a) Casey, P. C.; O'Connor, J. M. *Organometallics* **1985**, *4*, 384. (b) Merola, J. S.; Kacmarcik, R. T.; Engen, D. V. *J. Am. Chem. Soc.* **1986**, *108*, 329. (c) Rerek, M. E.; Bassolo, F. *J. Am. Chem. Soc.* **1984**, *106*, 5908. (d) Basolo, F. *Inorg. Chim. Acta* **1985**, *100*, 33. (e) King, R. B.; Efraty, A. *J. Organomet. Chem.* **1970**, *23*, 527.

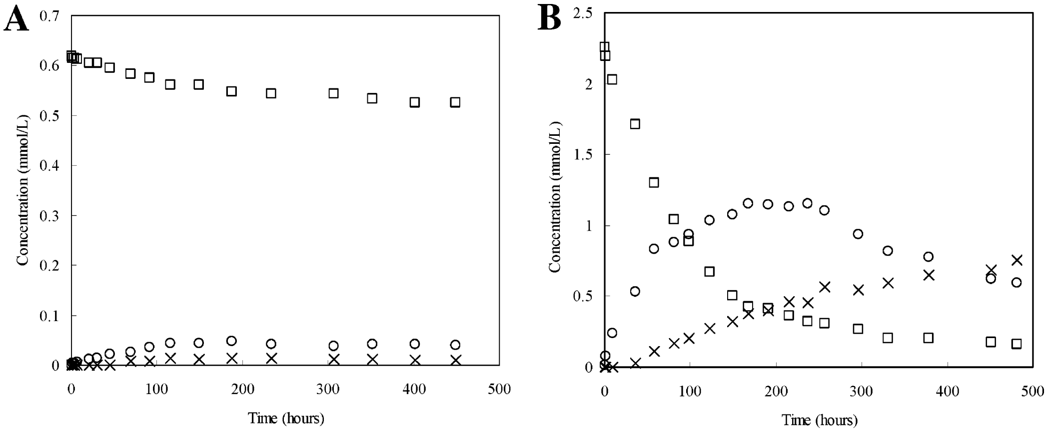

Figure 6. Exchange reaction from $\mathbf{1}_r$ with (A) 1.9 equiv of NEt_3; (B) 1.3 equiv of $CHCl_3$ (□: $\mathbf{1}_r$, ○: $\mathbf{1}_m$, ×: $\mathbf{1}_X$).

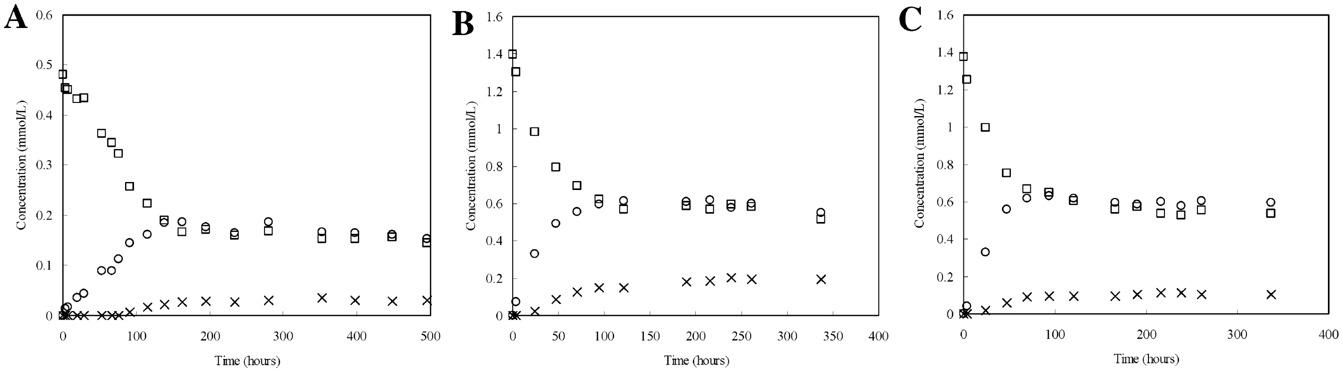

Figure 7. Exchange reaction from $\mathbf{1}_r$ with BHT: (A) 1 equiv, (B) 2.4 equiv, (C) 4.8 equiv (□: $\mathbf{1}_r$, ○: $\mathbf{1}_m$, ×: byproduct $\mathbf{1}_X$).

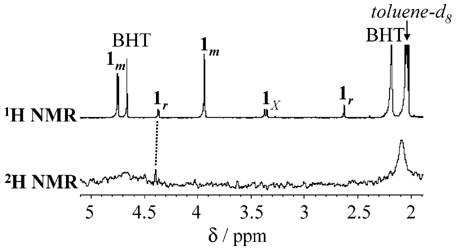

Figure 8. ^{1}H NMR (top) and ^{2}H NMR (bottom) spectra.

intermediates. Its formation requires a symmetrization by migration of silicon to C2 on both indenyl groups. This mechanism also explains the preferential generation of $\mathbf{1}_X$ from $\mathbf{1}_m$. There is significantly less molecular motion necessary to achieve the final geometry $\mathbf{1}_X$ starting from **5** than from **3** (Scheme 3).

Toluene was used as the solvent for all reactions. The distribution of reaction products greatly depended on the conditions. Bases inhibited both the interconversion of stereoisomers and the formation of side products (Figure 6A). Strong acids led to decomposition (Figure 6B; approximately 40% of the starting materials decomposed into products other than $\mathbf{1}_m$, $\mathbf{1}_r$, or $\mathbf{1}_X$). By contrast, with weak acids, side reactions are largely suppressed and the interconversion of $\mathbf{1}_r \rightleftharpoons \mathbf{1}_m$ becomes the dominant reaction. At low concentrations of acid, the consumption of the acid catalyst by side reactions suppresses interconversion, and an equilibrium is not established, as seen in the reaction in toluene alone, or with THF: conversion varies from about 10 to 20% (Figure 4, Figure 5). However, if sufficient weak acid is present (H_2O, BHT as catalysts), the interconversion $\mathbf{1}_r \rightleftharpoons \mathbf{1}_m$ occurs with an equilibration constant $K \approx 1$ (Figure 7, Figure 9): final ratios of $\mathbf{1}_m$:$\mathbf{1}_r$:$\mathbf{1}_X$ of 0.45:0.45:0.1 were achieved in all the BHT cases, but the rate at which the equilibrium was reached was dependent on BHT concentration. When 1 equiv of water was utilized in the system of $\mathbf{1}_r$ in toluene-d_8 (Figure 9), the reaction was accelerated and led to a 1:1 ratio of $\mathbf{1}_r$:$\mathbf{1}_m$ after approximately 40 h. This result also supports the proposed mechanism, with the water acting as a weak acid and as a small, coordinative polar ligand.

The foregoing observations should be placed in the context of the careful kinetic studies of Curnow and colleagues, who showed that the *meso* and *racemic* isomers of bis(1-diphenylphosphino-η^5-indenyl)iron, **6**, undergo facile interconversion, even at ambient temperature. Their proposed mechanism (Scheme 4) involves decomplexation of an indenyl ligand with concomitant coordination through the exocyclic phosphine substituent.[40] Evidently, such a scenario cannot be operative in the present cases, for which there is no convenient donor fragment and for which the barrier to interconversion of the *meso* and *racemic* isomers is very much higher. Interestingly, the *meso* compound is strongly disfavored in **6** relative to its *racemic* counterpart, possibly because π-stacking of the indenyl ligands would require the two bulky diphenylphosphino moieties to collide with each other. This problem does not arise for the silicone-bridged *ansa* ferrocenes $\mathbf{1}_r$ and $\mathbf{1}_m$.

Copolymerization of 1 with Oligo-dimethylsiloxane. Attempts to copolymerize **1** and **2** with

---

[40] (a) Curnow, O. J.; Fern, G. M.; Hamilton, M. L.; Jenkins, E. M. *J. Organomet. Chem.* **2004**, *689*, 1897. (b) Curnow, O. J.; Fern, G. M. *Organometallics* **2002**, *21*, 2827. (c) Curnow, O. J.; Fern, G. M.; Hamilton, M. L.; Zahl, A.; van Eldik, R. *Organometallics* **2004**, *23*, 906.

Scheme 3. Possible Mechanism for the Transformation Reaction via Successive 1,5-Sigmatropic Shifts

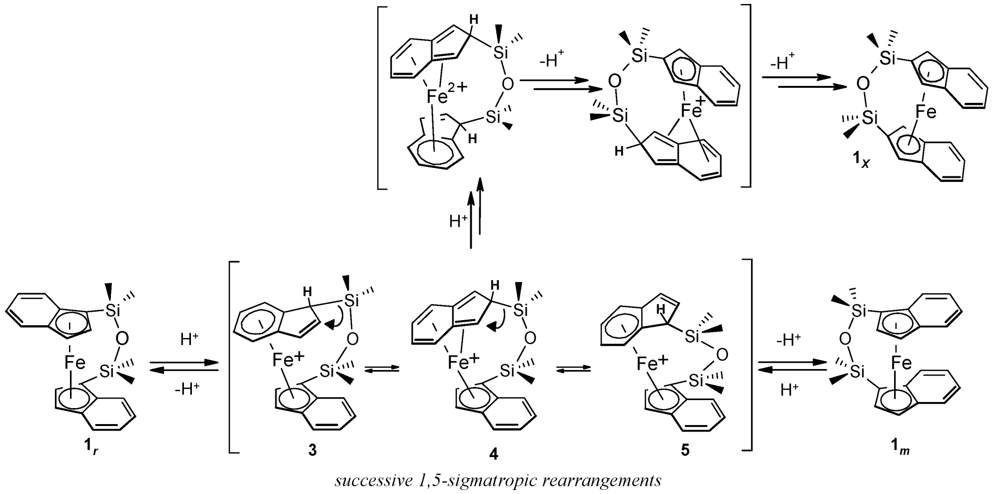

1,1,3,3,5,5,7,7-octamethylcyclotetrasiloxane (D_4) were performed under both acidic and basic conditions using trifluoromethanesulfonic acid and CsOH as the acidic and basic catalysts, respectively. The cesium hydroxide was dried by melting with a heat gun under vacuum to remove moisture, and reagents were then added. Compound **2** did not polymerize under either set of conditions: in both cases, all the D_4 was recovered and the majority of **2** remained in the flask. That is, metal-free **2** suppressed both acidic and basic catalysis of D_4 polymerization and redistribution. As previously noted, **1** decomposed under acidic conditions, especially with stronger acids. It was, therefore, not surprising that the attempt to copolymerize **1** with D_4 under catalysis by triflic acid led only to decomposed **1** and recovered D_4. However, the base-catalyzed copolymerization of metal-containing **1** with D_4 produced a highly viscous green-colored gum polymer.

Standard redistribution polymerization was also performed with **1**, D_4, and octamethyltrisiloxane (MDM). Initially, crystalline compounds $\mathbf{1}_r$ and $\mathbf{1}_m$ were used, but their solubilities were too low to reach equilibrium conditions overnight, as indicated by GPC and ^{1}H NMR: crystalline solids were found on the flask bottom. The copolymerization of **1**, which was initially dissolved in ether to avoid the above-noted solubility problem, followed by removal of ether, catalyzed by CsOH at 145 °C overnight, and followed by CO_2 neutralization, was performed to produce green, homogeneous polymers **10a**. The analogous cyclopentadienyl compound Fe(η^5-CpSiMe$_2$)$_2$O, **11**, was also prepared and copolymerized by the same method to produce an orange-color polymer **10b** (Scheme 5).

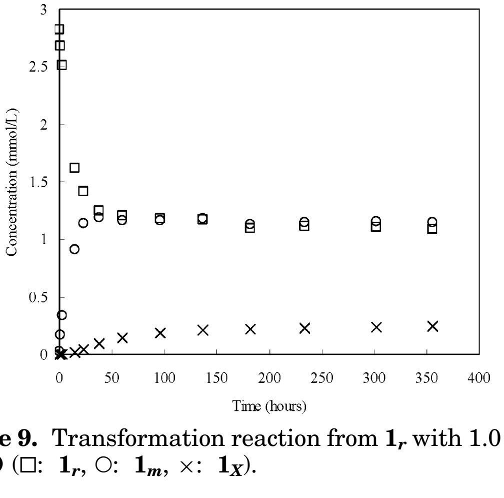

Figure 9. Transformation reaction from $\mathbf{1}_r$ with 1.0 equiv of H_2O (□: $\mathbf{1}_r$, ○: $\mathbf{1}_m$, ×: $\mathbf{1}_X$).

Scheme 4. Proposed Ring-Slippage Isomerization Process of Bis(1-diphenylphosphino-η^5-indenyl)iron by Curnow et al.[40]

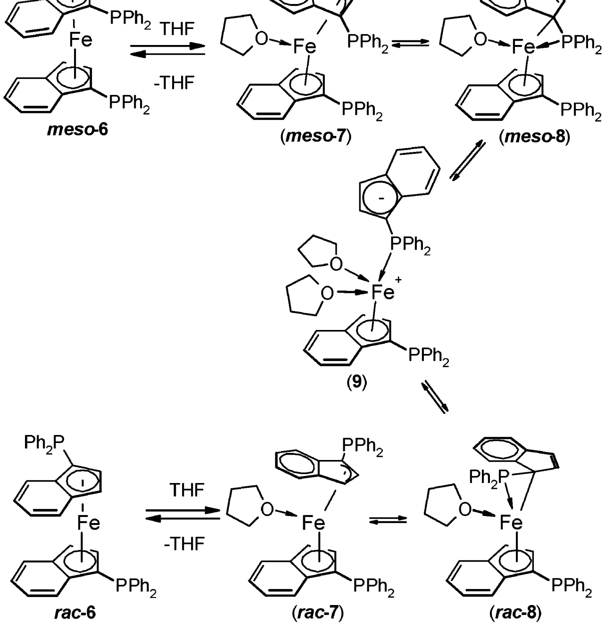

Compounds **10a** and **10b** were characterized by ^{1}H and ^{29}Si NMR and GPC using poly(dimethylsiloxane) standards. From the NMR analysis, only a small amount of the starting material remained. Both polymers showed bimodal signals (ca. 90 area %: 10 area %), as is the case with the normal equilibrium polymerization of poly(dimethylsiloxane)s. The lower intensity, lower molecular weight signals were assigned to oligocyclosiloxanes. The number average molecular weights of **10a** and **10b** were 6320 and 6010, respectively, comparable to the expected molecular weights, 6711 and 6354, respectively. The ^{29}Si NMR of **10a** showed a broad signal at 1.6 ppm for the *ipso*-Si atom of the indenyl rings, 7.3 ppm for the terminal Me$_3$*Si*-O

Scheme 5. Copolymerization of Either 1 or 11 with D_4 and MDM

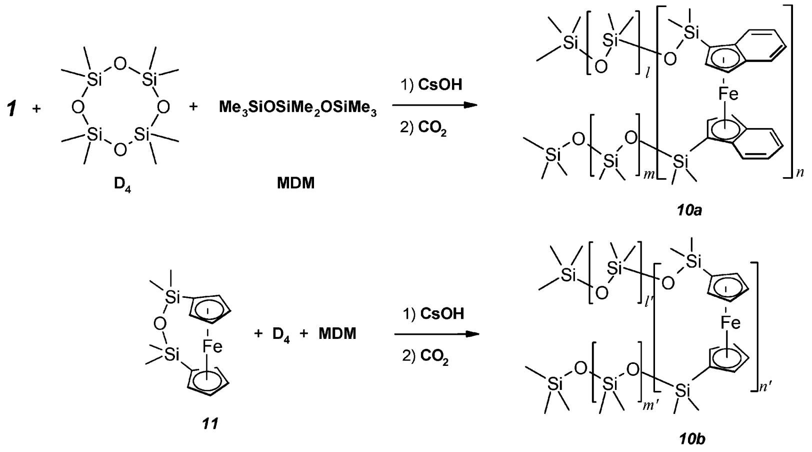

groups, and −19 to −22 ppm for the $-OSi Me_2O-$ groups. These GPC and ^{29}Si NMR data are consistent with the incorporation of the *ansa*-metallocene species into standard silicone polymer chains. The use of indenyl ligands permits the incorporation of ferrocenyl groups (but not of the metal-free ligands) under milder conditions than the analogous Cp-modified ligands.[12] Standard, mild methods with typical monomers D_4 and MDM may be used to prepare metal-containing poly(dimethylsiloxane)s without the need to resort to low loading of bulky functional compound, **1** or **11**.

Conclusions

Diastereomers of disiloxane-bis(1-indenyl)-*ansa*-ferrocenes, Fe(η^5-inden-1-yl-SiMe$_2$)$_2$O, $\mathbf{1}_r$ and $\mathbf{1}_m$, were prepared and characterized by a single-crystal X-ray diffraction study confirming the structure of each stereoisomer, *racemic* $\mathbf{1}_r$ and *meso* $\mathbf{1}_m$, resulting from the coordination of two indenyl ligands to the Fe metal centers. These isomers are also fully characterized by ^1H, ^{13}C, and ^{29}Si NMR, $^1H-^1H$ COSY, $^1H-^{29}Si$ HMBC, $^1H-^{13}C$ HSQC, and $^1H-^{13}C$ HMBC, and IR spectroscopy. These stereoisomers $\mathbf{1}_r$ and $\mathbf{1}_m$ underwent interconversion reactions that were retarded by basic conditions, but accelerated in acid. The mechanism of this process was investigated by a deuterium label experiment, and its result is consistent with a mechanism involving two successive Si−indenyl bond 1,5-sigmatropic rearrangements following protonation. Compound **1** was also copolymerized with D_4 and MDM to produce a green-colored organometallic polymer.

Experimental Section

General Procedures. All experiments for synthesizing organic compounds and organometallic compounds were carried out under nitrogen and argon atmosphere, respectively. All organometallic compounds were handled using Schlenk techniques.

Compounds. 1,3-Dichloro-1,1,3,3-tetramethyldisiloxane was purchased from ABCR; it was freshly distilled before use. Anhydrous iron(II) chloride was purchased from Alfa Aesar. Indene was obtained from BDH. Ferrocene, toluene-d_8, 1.6 N *n*-BuLi hexanes solution, Na, 2,6-di-*tert*-butyl-4-methylphenol, phenol, and 2,4,6-trimethylphenol were purchased from Aldrich. Reagent grade toluene, anhydrous grade THF, and anhydrous grade diethyl ether were dried over sodium-benzophenone ketyl and stored under a nitrogen atmosphere. Distilled grade acetone was dried over calcium sulfate and stored under a nitrogen atmosphere. Distilled grade methylene chloride was dried over calcium hydride and stored under a nitrogen atmosphere. Anhydrous grade hexanes, anhydrous *n*-hexane, anhydrous cyclohexane, and anhydrous grade *n*-heptane were purchased from Aldrich and used as received.

Equipment. IR spectra were recorded on a Perkin-Elmer 283 dual-beam spectrometer. ^1H, ^2H, ^{13}C, and ^{29}Si NMR spectra were recorded on Bruker AV600, Bruker AV300, and Bruker AV200 Fourier transform spectrometers with tetramethylsilane as internal and external standard. Elemental analyses were performed by Guelph Chemical Laboratories Ltd. Mass spectra were performed by the McMaster Regional Centre for Mass Spectrometry. Electron impact (EI) and chemical ionization (CI, NH_3) mass spectra were recorded at 70 eV with a source temperature of 200 °C on a "Micromass GCT" mass spectrometer using a heated probe. High-resolution mass spectral (HRMS) data were obtained using the EI method calibrant with perfluorotributylamine. GPC equipment consisted of a Waters 515 pump, a Waters 717 autosampler, and a Waters 2410 differential refractometer. The separation was made with two Polymer Laboratories PLgel 5 μm Mixed-C columns, preceded by a PLgel 5 μm guard column. The analyses were performed using HPLC grade toluene flowing at 1.0 mL/min as the eluent, and the columns and detector were both heated to 45 °C. The samples were prepared in toluene at 0.5% w/v polymer and transferred to glass autosampler vials without filtering. An injection volume of 50 μL was used, and data were collected for 25 min. Data collection and analyses were performed using ThermoLabsystems Atlas chromatography software and Polymer Laboratories Cirrus GPC software. Molecular weight averages were determined relative to a calibration curve (3rd order) created using poly(dimethylsiloxane) standards.

X-ray Crystallography. X-ray crystallographic data for $\mathbf{1}_r$ (CDCC 252723) and $\mathbf{1}_m$ (CDCC 252722)[41] were collected from single-crystal samples, each mounted on a glass fiber. Data were collected using a P4 Siemens diffractometer, equipped with a Siemens SMART 1K charge-coupled device (CCD) area detector (using the program SMART[42]) and a rotating anode using graphite-monochromated Mo Kα radiation ($\lambda = 0.71073$ Å) at 173 K. Processing was carried out "Ronald Kluger" <rkluger@chem.utoronto.ca> using the program SAINT,[43] which applied Lorentz and polarization corrections to three-

---

(41) CCDC 252722 and 252723 contain the supplementary crystallographic data for this paper. These data can be obtained free of charge via www.ccdc.cam.ac.uk/data_request/cif, by e-mailing data_request@ccdc.cam.ac.uk, or by contacting The Cambridge Crystallographic Data Centre, 12 Union Road, Cambridge CB2 1EZ, UK; fax: +44 1223 336033.

(42) Sheldrick, G. M. *SMART*, Release 4.05; Siemens Energy and Automation Inc.: Madison, WI, 1996.

Table 4. Attempted E/Z Transformation Reactions[a]

compound	quantity	reagent	quantity	reaction time	figure
$\mathbf{1}_r$	1.4 mg	BHT	0.9 mg (1.0 equiv)	1 month	Figure 7A
$\mathbf{1}_r$	4.0 mg	BHT	4.4 mg (2.4 equiv)	1 month	Figure 7B
$\mathbf{1}_r$	4.0 mg	BHT	8.7 mg (4.8 equiv)	1 month	Figure 7C
$\mathbf{1}_m$	4.8 mg	*d*-BHT	7.0 mg (2.7 equiv)	1 month	Figure 3S[c]
$\mathbf{1}_r$	1.8 mg	NEt_3	1.2 μL (1.9 equiv)	1 month	Figure 6A
$\mathbf{1}_r$	2.5 mg	THF	1.5 μL (2.7 equiv)	1 month	Figure 5
$\mathbf{1}_r$	6.6 mg	$CHCl_3$	1 μL (1.3 equiv)	1 month	Figure 6B
$\mathbf{1}_r$	8.3 mg	H_2O	0.37 μL (1.0 equiv)[b]	1 month	Figure 9

[a] Each equivalent ratio of reagents was calculated by the integral ratio in ^{1}H NMR spectra. The sealed NMR tubes were placed in an oil bath at 110 °C, and ^{1}H NMR spectra were recorded at room temperature. [b] Equivalent ratio of H_2O was calculated by the added amount of each compound, $\mathbf{1}_r$ and H_2O. [c] See Supporting Information.

dimensional integrated diffraction spots. The program SADABS[44] was utilized for the scaling of diffraction data, the application of a decay correction, and an empirical absorption correction based on redundant reflections. Both crystal structures were solved by using the direct methods procedure in the Bruker SHELXTL[45] program library. Unconstrained refinement was carried out by using full-matrix least-squares methods with anisotropic thermal parameters for all nonhydrogen atoms. Hydrogen atoms were added at calculated positions for $\mathbf{1}_r$ and were refined using a riding model, with the positions and isotropic temperature factors tied to the bonded carbon atoms. For the larger $\mathbf{1}_m$ crystal, the hydrogen atoms were found by difference Fourier methods and refined isotropically. Minor extinction corrections of 0.00018(7) ($\mathbf{1}_r$) and 0.0023(6) ($\mathbf{1}_m$) were applied.

Syntheses. 1,3-Bis(1-indenyl)-1,1,3,3-tetramethyldisiloxane, 2. Indene was freshly distilled (clear transparent liquid) as a fraction from 90−98 °C/15−25 mmHg. Indene (14.70 g, 1.2655 × 10^{-1} mol) was dissolved in THF (180 mL) and cooled to −78 °C. *n*-BuLi (1.6 N in hexanes solution, 79 mL, 1.264 × 10^{-1} mol) was added dropwise over 20 min. In the course of the reaction, the color changed to give a yellow suspension. After addition, the flask was gradually heated to room temperature to produce a transparent orange solution. The solution was again cooled to −78 °C (yellow suspension). Freshly distilled 1,1,3,3-tetramethyl-1,3-dichlorodisiloxane (clear transparent liquid, 12.86 g, 6.327 × 10^{-2} mol) was added dropwise into the flask. The color gradually changed from a yellow suspension to orange transparent then to pale yellow transparent solution. The flask was gradually heated to room temperature and stirred overnight, then the solvents were distilled off and the product was distilled by use of a microdistillation oven to produce a clear transparent liquid (135−140 °C/1 mmHg, 2 diastereomers). Yield: 13.726 g (59.8% yield). ^{1}H NMR ($CDCl_3$): δ −0.12 (s, 6H, Si*Me*), −0.11 (s, 6H, Si*Me′*), −0.05 (s, 6H Si*Me*), −0.04 (s, 6H, Si*Me′*), 3.49 (s, 2H), 6.60 (m, 2H), 6.93 (d, *J* = 5.4 Hz, 2H), 7.21 (m, 4H), 7.46 (m, 4H). ^{13}C NMR ($CDCl_3$): δ 144.4, 144.1, 134.8, 129.6, 124.9, 123.7, 123.0, 121.0, 48.2, −1.0. ^{29}Si NMR ($CDCl_3$, 59.6 MHz, rt): δ 5.64. IR (KBr, cm^{-1}): 3065, 2958, 2898, 1717, 1605, 1536, 1458, 1450, 1390, 1360, 1256, 1067, 1040, 1025, 977, 829, 793, 777. Mass spectra (calcd *m/z* 362) (EI, *m/z*): 247 (M^+ − Indenyl); (CI, *m/z*): 380 ($M^+ + NH_4$).

Fe(η^5-Inden-1-yl-SiMe$_2$)$_2$O, 1. 1,3-Bis(1-indenyl)-1,1,3,3-tetramethyldisiloxane (3.623 g, 9.990 × 10^{-3} mol) and TMEDA (3.02 mL, 2.00 × 10^{-2} mol) were dissolved in anhydrous *n*-hexanes (45 mL) and cooled to −78 °C. *n*-BuLi (1.6 N in hexanes solution, 12.5 mL, 2.0 × 10^{-2} mol) and hexanes (15 mL) were added dropwise over 3 min. After addition, the flask was gradually heated to room temperature and stirred overnight. The solvent was distilled off in vacuo. Then, THF (50 mL) was added and the solution was cooled to −78 °C, $FeCl_2$ (1.215 g, 9.586 × 10^{-3} mol) was added, and the solution was allowed to warm to ambient temperature. The solvents were distilled off in vacuo, and resulting residual solid was dissolved in diethyl ether and filtered through Celite. The solvents were removed in vacuo to produce a dark brown compound (3.470 g). The compound was purified using Al_2O_3 column chromatography with anhydrous hexanes as an eluent. Green and blue fractions were collected (earlier fractions mainly consisted of the *racemic* isomer and later fractions mainly consisted of the *meso* isomer). Each was recrystallized from *n*-heptane to produce black and dark red crystals, respectively. Yield: total 0.6383 g (1.533 × 10^{-3} mol, 16.0%). ^{1}H NMR (toluene-d_8): $\mathbf{1}_r$: δ 0.50 (s, 6H), 0.58 (s, 6H), 2.68 (d, *J* = 2.5, 2H), 4.42 (dd, *J* = 2.5, 0.7 Hz, 2H), 6.87 (m, 4H), 7.64 (m, 2H), 7.69 (m, 2H), $\mathbf{1}_m$: δ 0.41 (s, 6H), 0.52 (s, 6H), 3.99 (d, *J* = 2.5 Hz, 2H), 4.80 (d, *J* = 2.5 Hz, 2H), 6.50 (m, 2H), 6.70 (m, 2H), 6.73 (m, 4H). ^{13}C NMR (CD_2Cl_2): $\mathbf{1}_r$: δ 0.7 (q, $^1J_{CH}$ = 118 Hz, Si*Me*), 1.4 (q, $^1J_{CH}$ = 118 Hz, Si*Me*), 64.6 (s), 81.1 (d, $^1J_{CH}$ = 180 Hz), 67.8 (d, $^1J_{CH}$ = 176 Hz, C*H*), 87.4 (s), 90.4 (s), 131.2 (d, $^1J_{CH}$ = 162 Hz, C*H*), 124.2 (d, $^1J_{CH}$ = 159 Hz, C*H*), 124.6 (d, $^1J_{CH}$ = 159 Hz, C*H*), 130.0 (d, $^1J_{CH}$ = 163 Hz, C*H*), $\mathbf{1}_m$: δ 1.4, 63.0, 75.7 (d, $^1J_{CH}$ = 174 Hz), 64.7 (d, $^1J_{CH}$ = 176 Hz), 90.6, 92.1, 126.4, 122.3, 122.6, 125.3. ^{29}Si NMR ($CDCl_3$, 59.6 MHz, rt): $\mathbf{1}_r$: δ 1.32, $\mathbf{1}_m$: δ 1.60. IR (KBr, cm^{-1}): $\mathbf{1}_r$: 3080, 3050, 3013, 2962, 1620, 1456, 1389, 1336, 1299, 1251, 1144, 1016, 827, 787, 750, $\mathbf{1}_m$: 3080, 3043, 3013, 2960, 1632, 1456, 1387, 1334, 1300, 1252, 1140, 1023, 1006, 828, 793. Mass spectra (calcd *m/z* 416.1) $\mathbf{1}_r$, EI: 416.1 (M^+); CI: 416.1 (M^+), $\mathbf{1}_m$, EI: 416.1 (M^+); CI: 416.1 (M^+). Anal. Calcd for $C_{22}H_{24}OFe_2Si_2$: C, 63.45; H, 5.81. Found: $\mathbf{1}_r$: C, 63.33; H, 5.69, $\mathbf{1}_m$: C, 63.58; H, 5.81.

Fe(η^5-CpSiMe$_2$)$_2$O, 11. 11 was synthesized according to the published procedure.[12] Dilithioferrocene-tetramethylenediamine[46] (4.20 g, 13.4 mmol) was suspended in ether (40 mL) and THF (20 mL) at −78 °C, then 1,3-dichloro-1,1,3,3-tetramethyldisiloxane (2.62 mL, 13.4 mmol) was added dropwise. The solution was gradually warmed to room temperature, allowed to stir overnight at ambient temperature, and filtered off through Celite over a glass filter to remove the lithium chloride byproduct. Purification was achieved using alumina/hexanes column chromatography. Elution with a 95:5 mixture of hexane−ether gave an orange band that was separated and recrystallized from hexanes to yield the crystalline product (1.63 g, 3.2 mmol, 24% yield). ^{1}H NMR ($CDCl_3$): δ 0.26 (s, 12H), 4.05 (m, 4H), 4.20 (m, 4H). ^{13}C NMR ($CDCl_3$): δ 1.4, 71.4, 71.5, 72.9. ^{29}Si NMR ($CDCl_3$): δ 0.3. IR (KBr, cm^{-1}): 3093, 2959, 2901, 1635, 1423, 1365, 1253, 1168, 1038, 817, 788.

***E/Z* Transformation Reactions.** Crystal $\mathbf{1}_r$ and $\mathbf{1}_m$ were charged into NMR tubes, respectively, and the atmosphere in the tubes was replaced with argon three times. Then, the tube was charged with distilled toluene-d_8 (0.7 mL), followed by freezing deaeration with a dry ice−acetone bath. Then each chemical was added, respectively, under an argon atmosphere (Table 4), followed by sealing with a flame.

---

(43) Sheldrick, G. M. *SAINT*, Release 4.05; Siemens Energy and Automation Inc.: Madison, WI, 1996.

(44) Sheldrick, G. M. *SADABS* (Siemens Area Detector Absorption Corrections), 1996.

(45) Sheldrick, G. M. *Siemens SHELXTL*, Version 5.1; Siemens Crystallographic Research Systems: Madison, WI, 1998.

(46) Butler, I. R.; Cullen, W. R.; Ni, J.; Rettig, S. J. *Organometallics* **1985**, *4*, 2196.

Copolymerization. Copolymerization of Fe(η^5-Inden-1-yl-SiMe$_2$)$_2$O with Oligosiloxanes under Basic Conditions. $\mathbf{1}_{\boldsymbol{r}}$ with D$_4$ and MDM: A 25 mL round-bottomed flask with CsOH was dried by heating with a heat gun under vacuum (0.0094 g, 6.3×10^{-5} mol after drying). Then, $\mathbf{1}_{\boldsymbol{r}}$ (4.0 mg, 9.6×10^{-6}mol), D$_4$ (0.930 g 3.13×10^{-3} mol), and MDM (0.078 g, 3.3×10^{-4} mol) were added in the flask, which was then heated at 150 °C for 15 h. The flask was cooled to room temperature and neutralized by CO$_2$ gas. Crystals plus an amorphous, clear solid were formed. ^{1}H NMR (C$_6$D$_6$) showed only Si*Me*'s signals at δ 0.20 and 0.28, and no indenyl ligand signals. This is consistent with a polymerization in which $\mathbf{1}_{\boldsymbol{r}}$ did not participate.

GPC (g/mol) peak 1; 77.9 area %: M_n: 3.81×10^3, M_w: 6.57×10^3, M_z: 1.00×10^4, peak 2; 22.1 area %: M_n: 4.28×10^2, M_w: 4.44×10^2, M_z: 4.63×10^2.

$\mathbf{1}_{\boldsymbol{m}}$ with D$_4$ and MDM: A 25 mL round-bottomed flask with CsOH was dried by heating with a heat gun under vacuum (0.0053 g, 3.5×10^{-5} mol after drying). Then, $\mathbf{1}_{\boldsymbol{m}}$ (2.6 mg, 6.2×10^{-6} mol), D$_4$ (0.972 g, 3.28×10^{-3} mol), and MDM (0.125 g, 5.27×10^{-4} mol) were added in the flask, which was then heated at 150 °C for 15 h. The flask was cooled to room temperature and neutralized by CO$_2$ gas. Then they were heated at 150 °C for 15 h, followed by cooling to room temperature and neutralizing by CO$_2$ gas. As with $\mathbf{1}_{\boldsymbol{r}}$, the product polymer contained no indenyl groups.

GPC (g/mol) peak 1; 76.6 area %: M_n: 2.80×10^3, M_w: 4.40×10^4, M_z: 6.41×10^3, peak 2; 23.4 area %: M_n: 4.27×10^2, M_w: 4.45×10^2, M_z: 4.65×10^2.

Racemic, compound **1** (powder) as a starting material: **1** (0.245 g, 5.89×10^{-4} mol) was dissolved into ether in a Schlenk flask. The ether was removed under vacuum, and D$_4$ (4.546 g, 1.53×10^{-2} mol) and MDM (0.175 g, 7.40×10^{-4} mol) were added to generate a dark green solution. CsOH was dried by heating with a heat gun under vacuum in a different flask (0.071 g, 4.76×10^{-4} mol after drying), to which the siloxanes and **1** were added; the mixture was heated at 145 °C for 11 h. The flask was cooled to room temperature, then CO$_2$ gas was bubbled under the mixture and was neutralized. Hexanes (20 mL) was added, and after filtration through Celite over a glass filter to remove a salt, the solvents were removed to give dark green viscous liquid **10a**. Yield: 4.250 g (85.6%). ^{1}H NMR (CDCl$_3$): δ −0.2 to 0.6 (Si*Me*), 2.8−3.0 (br), 3.4 (br), 4.0−4.1 (br), 4.1−4.2 (br), 4.5−4.7 (br), 4.7−4.9 (br), 4.9−5.1 (br), 6.4−7.9 (br). ^{29}Si NMR (CDCl$_3$): δ 7.3, 6.2 (very small signal), 5.4 (very small signal), 1.6, −19.1, −21.9 (−20.4 to −22.5). IR (KBr, cm^{-1}): 2965, 2907, 1605, 1449, 1412, 1261, 1086, 1027, 863, 805. GPC (g/mol) peak 1; 89.8 area %: M_n: 6.32×10^3, M_w: 1.18×10^4, M_z: 1.78×10^4, peak 2; 10.2 area %: M_n: 4.77×10^2, M_w: 4.95×10^2, M_z: 5.16×10^2.

Copolymerization of Fe(η^5-CpSiMe$_2$)$_2$O, 11, with Oligosiloxanes under Basic Conditions. A Schlenk flask was charged with CsOH, which was dried by heating with a heat gun (0.109 g, 7.29×10^{-4} mol after drying). **11** (0.171 g, 5.41×10^{-4} mol), D$_4$ (2.333 g, 7.86×10^{-3} mol), and MDM (0.096 g, 4.08×10^{-4} mol) were added to the flask to generate an orange solution. It was heated at 145 °C for 11 h. The flask was cooled to room temperature, then CO$_2$ gas was bubbled for neutralization. Hexanes (10 mL) was added, and the solution was filtered through Celite over a glass filter to remove salt, followed by removal of solvents to generate a viscous orange liquid, **10b**. Yield: 1.716 g (66.0%). ^{1}H NMR (CDCl$_3$): δ 0.05−0.15 (br, Si*Me*), 3.97−4.38 (br m). ^{13}C NMR (CDCl$_3$): δ 68.0 68.4, 70.9, 71.2, 71.7, 72.9, 73.0, 73.4. ^{29}Si NMR (CDCl$_3$): δ 7.1, 0.1, −0.1, −19.1, −21.9(−21.3 to −22.5). IR (KBr, cm^{-1}): 2965, 2907, 1602, 1445, 1413, 1261, 1092, 1027, 863, 805. GPC (g/mol) peak 1; 93.8 area %: M_n: 6.01×10^3, M_w: 1.34×10^4, M_z: 2.54×10^4, peak 2; 6.2 area %: M_n: 4.84×10^2, M_w: 5.03×10^2, M_z: 5.22×10^2.

Copolymerization of 2 with Oligosiloxanes under Basic Conditions. An attempt to copolymerize **2** with D$_4$ under basic conditions with CsOH was performed by a procedure similar to that above for **10a** and **10b**. **2** (1.39 g, 3.84×10^{-3} mol), D$_4$ (14.2 g, 4.79×10^{-2} mol), and CsOH (0.0156 g, 5.73×10^{-5} mol) were charged in a 50 mL round-bottomed flask that was then heated at 100 °C for 9 h. Black solids precipitated, but no polymerization was found by gas chromatography. The flask was heated at 140 °C for a further 8 h; again no polymer was observed by GC. After acidifying with acetic acid (3 drops) and removal of the volatiles by distillation, **2** was collected.

Copolymerization of 2 with Oligosiloxanes under Acidic Conditions. An attempt to copolymerize **2** with D$_4$ under the acidic conditions using trifluoromethanesulfonic acid (FC-24) was performed by a procedure similar to that above for **10a** and **10b**. **2** (1.39 g, 3.84×10^{-3} mol), D$_4$ (14.2 g, 4.79×10^{-2} mol), and FC-24 (11.0 μL, 1.24×10^{-4} mol) were charged in a 50 mL round-bottomed flask that was heated at 100 °C for 9 h. No evidence for polymerization was found by gas chromatography even after further heating at 140 °C for 8 h. After neutralization with triethylamine (2 drops) followed by distillation of the volatiles under vacuum conditions, **2** was re-collected.

Acknowledgment. We thank Dow Corning Toray Silicone Co., Ltd. and Dow Corning Corporation for financial support and GPC analysis.

Supporting Information Available: 2D NMR spectra, including ^{1}H NOE experiments and ^{1}H−^{29}Si HMBC spectra of $\mathbf{1}_{\boldsymbol{r}}$ (27%) and $\mathbf{1}_{\boldsymbol{m}}$ (73%) and a detailed description of ^{1}H−^{13}C gradient HSQC spectra of $\mathbf{1}_{\boldsymbol{r}}$ (27%) and $\mathbf{1}_{\boldsymbol{m}}$ and CIF files for $\mathbf{1}_{\boldsymbol{r}}$ and $\mathbf{1}_{\boldsymbol{m}}$. This information is available free of charge via the Internet at http://pubs.acs.org.

OM0491847